Behavior of conducting polymer-based micro-actuators under a DC voltage

L. Seurre, H. Aréna, Sofiane Ghenna, Caroline Soyer, Sébastien Grondel, Cedric Plesse, G.T.M. Nguyen, F. Vidal, Eric Cattan

Behavior of conducting polymer-based micro-actuators under a DC voltage

L. Seurre[a], H. Aréna[a], S. Ghenna[a], C. Soyer[a], S Grondel[a], C. Plesse[b], G.T.M. Nguyen[b], F. Vidal[b], E. Cattan[a]

[a]Univ. Polytechnique Hauts-de-France, CNRS, Univ. Lille, Yncrea, Centrale Lille, UMR 8520 - IEMN, DOAE, F-59313 Valenciennes, France ;

[b]CY Cergy Paris Université, LPPI, F95000 CERGY, France.

Keywords: Electroactive polymer, electronically conducting polymer, residual strain, back-relaxation, DC voltage

corresponding author: eric.cattan@uphf.fr

Abstract

Conducting polymer-based micro-actuators are of great interest in soft MEMS as they exhibit large strains and forces in response to electrical stimulation. To date, these micro-actuators have very often been characterized by applying low frequency voltage to extract the electromechanical characteristics. However, many applications require maintaining the actuator's position for several minutes. A micro-camera tracking the displacements of an object, the actuation of a cochlear implant during surgery, or closing micro-tweezers to manipulate objects are potential applications for which actuation is achieved by applying a direct current (DC) voltage. Knowledge of the behavior of micro-actuators under and after a DC voltage is crucial for modeling and future control. Consequently, the kinetics to reach the maximum strain followed by back-relaxation are identified and discussed. It is shown that it is the result of competition between an elastic restoring force and the backflow of the ions inside the actuator. A residual strain is observed after a short circuit or an open circuit and studied as a function of the voltage applied. It is demonstrated that the voltage and the chronology of the power-ups affect the actuator position and strain amplitude. The interpretation of the experimental results linked directly to the intrinsic operation of micro-actuators is presented.

1. Introduction

The electromechanical performance of ionic electroactive polymers (i-EAPs) is usually studied using a square-wave voltage applied at low frequencies between 0.01 Hz and around 20 Hz allowing time for the ions to move in one direction and then the other to maximize the strain. Beyond these frequencies, the strain decreases drastically until it disappears due to the intrinsic mode of operation of these actuators [1][2]. However, the low frequencies are not the operating mode of the actuators involved in some applications. A direct current (DC) signal or a set voltage level is sometimes tuned to obtain the desired position of the actuator by moving in one direction and maintaining the position for a few minutes. Understanding their working mechanisms under a DC voltage and when the voltage is cut off is becoming increasingly important to improve the development and control of microdevices. Consequently, data on the dynamics of the actuator under/after a DC voltage to reach a strain difference (SD) set point or its maximum are useful for future applications.

Among i-EAPs, ionic polymer-metal composites (IPMCs) have been described under a DC voltage and the most important physical phenomenon associated with IPMC actuation is the back-relaxation of the actuator. IPMCs comprise a cation exchange membrane (ionomeric polymer membrane) sandwiched between metal electrodes. The membrane consisted of the anions that are covalently fixed to the

polymer backbone is electrically neutralized with counter-cations. Redistribution of the cations and the adjacent water molecules occurs when a voltage is applied, which is generally regarded as the key physical driver of IPMC actuation [3][4]. Back-relaxation is described in several studies for a range of material compositions (cation and solvent type) and experimental conditions such as the degree of hydration, applied voltage, and in-air versus in-solvent testing [5][6][7][8][9][10][11][12][13][14][15][16][17]. The composite bends to the anode side, for example, and gradually bends back to the cathode side while still under an electric potential. The generally accepted view of the underlying physical mechanisms of back-relaxation focuses on the slow flow of water within the ionomer [18]. Specifically, as the cations migrate toward the cathode they rapidly carry the water molecules attached to them but also drag along excess free water within the ionomer. This is similar to the "added mass" effect in fluid mechanics. Once carried toward the cathode, the free water slowly diffuses back into the ionomer causing the IPMC to relax under an applied voltage. Back-relaxation in saturated Nafion samples was observed for a large number of alkali metal cations but was found to be abolished for large organic cations [6] resulting in weaker, slower actuation. The level of hydration was also shown to play a central role in back-relaxation whereby the removal of a fraction of the water in the ionomer can be used to reduce the phenomenon [8]. In [16], the authors created a small electrically isolated region in Pt layers with a specific pattern and applied two specific electrical fields simultaneously to restrain back-relaxation. These relaxation effects do not facilitate IPMC control to maintain the actuator in a static position [17]. Moreover, Y. Bar-Cohen *et al.* [11] indicated that remnant deformation was common in IPMC materials after being subjected to electrical activation. In [11], Flemion/TBA^+ samples remained deformed a long time after the voltage was brought to zero, which poses difficulties when attempting to examine the repeatability of the measurements.

Electronically conducting polymers (ECP) are a class of materials with a conjugated backbone structure exhibiting controllable electronic conductivities and are currently used to fabricate actuators operating in solution or air. Under a low applied voltage (less than 2V), oxidation or reduction creates delocalized positive charge carriers along the ECP backbone, and ions are inserted for maintaining the electroneutrality within ECP, inducing their dimensional changes inducing dimensional changes. These ions enter the polymer from the surrounding electrolyte and serve to balance the charge. These changes suggest that the intercalation of ions between the polymer chains is at least partly responsible for swelling [19][20][21][22][23].

For these materials, the studies on the dynamics of relaxation are focus on cyclic voltammetry measurements where the current as the potential and the sweep speed are varied. A change in the charge (oxidation) curve for polyaniline films was observed in [24] depending on the relaxation time of the ECP. The authors synthesized oxidized polyaniline films, waited between 10 s and 10 000 s for the ECP to relax to its reduced state, and then observed the resulting oxidation state using cyclic voltammetry with a sweep speed of 100 $mV.s^{-1}$. They observed that the longer the relaxation time is, the resulting anode current peak (oxidation of ECP) obtained by cyclic voltammetry is higher and sharper and shifts toward higher potentials. The authors explain that this situation is attributable to stronger attractions between species occurring during oxidation and reduction of the ECP during the relaxation phase, and/or through the redox reaction that can occur in two stages: firstly, the production of a polaron then a bipolaron. This team thus introduced the term "memory effect". In the literature, the concept of the memory effect appears regularly when the behavior of the actuator is disrupted depending on its electrochemical history. Furthermore, Otero *et al.* have conducted studies on the current, charge, and effect of maintaining the electrochemical state of the ECP over varying periods using polypyrrole (PPy) based actuators operating in solution [25] [26] [27]. The team has studied the effect of the holding time of PPy films in a reduced state [25]: The voltage was maintained at -2000 mV for varying periods (1 to 2981 s), then cyclic voltammetry was conducted between -2000 and +300 mV at a speed of 30 $mV.s^{-1}$. The same film was used and the voltage was held at 300 mV (oxidized state) for 5 min between each measurement to erase the film history. The authors observed that the longer the holding time in a reduced state, the more the oxidation peaks shifted toward more anodic values. From these results, they deduced that more intense reduction leads to the more

effective compaction due to the release of counterions and solvent molecules in the ECP. This indicates that the history of the film has not been totally wiped, probably due to the difficulty of the film to expand (oxidation) after being contracted for a long time (reduced state). According to their interpretations, the polymer structure of the film can be compacted (contracted ECP film) either by applying a high cathode potential or maintaining this potential for a long time and the film memorizes this structure (it remains partly contracted). They also observed that oxidation of a compacted structure does not wipe the structural memory, and this promotes the emergence of hysteresis in the electrochemical cycle of the film [26]. The memory effect has also been described for PPy films with pendant titanocene dichloride centers [28], where the variation in the current as a function of the applied voltage was dependent on the measurement parameters (variation of voltage extremes and sweep speed, interruption of the sweep at certain points). It has been established that both the electroactive components of the film, the polymer matrix and the immobilized centers, contribute to the memory effect. Sendai *et al.* [29] studied electro-chemo-mechanical strain under tensile stress in PPy films and discussed the results in terms of the relaxation of the anisotropic strain and the memory effect introduced during creeping. In sum, research has focused on relaxation under a continuous electric current for IPMC and on the study of the electrochemical history of the ECP using cyclic voltammetry for ECP-based actuators.

To our knowledge, there is very little applicable data to map the behavioral dynamics of conducting polymer-based actuators when a DC voltage is applied for several minutes. The objective of this paper is to identify the time-dependent correspondence between the transient input DC voltage and the shape of the conducting polymer-based actuators and propose some interpretations. First, the method used to fabricate the extremely small (35 µm thick with a surface area of a few square millimeters) trilayer actuators (PEDOT:PSS-PEO/NBR-PEO/ PEDOT:PSS-PEO) tested is described and their traditionally accepted mode of operation (redox process) is quickly explained. Then, a specific measuring protocol related to the need to apply successive electrical voltages with the same polarity is briefly presented. In this paper, the study focuses more on the dynamics of actuation under a DC voltage and the dynamics of relaxation after a short circuit. The effect of the voltage, according to the chronovoltamogram, on the strain difference, the residual strain difference, as well as the charge stored and restored was observed and analyzed. A resulting macroscopic explanation of the phenomenon is proposed.

2. Materials and methods

2.1. Materials

Poly(ethylene glycol) methyl ether methacrylate (PEGM, Mn = 500 g.mol^{-1}), poly(ethylene glycol) dimethacrylate (PEGDM, Mn = 750 g.mol^{-1}), ammonium persulfate (APS, 98 %), and cyclohexanone (>99.8 %) were obtained from Sigma Aldrich and used as received. Poly(3,4-ethylenedioxythiophene) polystyrene sulfonate (PEDOT:PSS) aqueous solution (Clevios PH1000, solid content 1.0 – 1.3 wt%) was purchased from Heraeus Precious Metals GmbH & Co. Nitrile butadiene rubber (NBR), initiator dicyclohexyl peroxydicarbonate (DCPD), and 1-ethyl-3-methylimidazolium bis(trifluoromethanesulfonyl)imide (EMImTFSI 99.9%) were used as supplied from LANXESS, Groupe Arnaud, and Solvionic, respectively.

2.2. Micro-actuator fabrication and measurement set-up

The trilayer actuators composed of a PEO-NBR ion storage membrane (ISM) sandwiched between two electroactive PEDOT:PSS-PEO layers were fabricated using the layer stacking method [30][31][32]. The PEDOT:PSS-PEO casting solutions were obtained by mixing PEO (poly(ethylene oxide)) precursors

(mPEG, methacrylic functionalized PEG) composed of 50 wt% PEGM and 50 wt% PEGDM as the monomer and the crosslinker, respectively, with an aqueous dispersion of PEDOT:PSS (40 wt% with respect to the final electrode, i.e. 60 wt% PEDOT:PSS, equivalent to 1.15 wt% solid content). APS was also added to the solution (3 wt% with respect to mPEG) as a radical initiator for the precursors. The solution was stirred until dissolution. The resulting solution was cast (0.05 ml.cm^{-2}) onto a glass slide and placed on a heating plate at 50°C to evaporate the water. The ion storage membrane located between the two polymer electrodes was based on a semi-interpenetrating polymer network layer composed of a PEO network (50 wt%) and linear NBR (50 wt%). First, the NBR solution was prepared by dissolving NBR in cyclohexanone to obtain a concentration of 20 wt%. The PEO precursors consisting of PEGDM (25 wt% with respect to the PEO network) and PEGM (75 wt% with respect to the PEO network) were added to the NBR solution and stirred for 30 min. The radical initiator DCPD (3 wt% with respect to the PEO network) was then added to the solution. The final solution was stirred until complete homogenization and degassed. During the next step, the reactive mixture was spin coated (3000 rpm – 1000 rpm/s – 30 s) onto the first PEDOT:PSS-PEO electrode layer and pre-polymerized in a closed annealing chamber under continuous nitrogen flow for 45 min at 50°C to initiate the formation of the PEO network. The second PEDOT:PSS-PEO electrode was fabricated on top of the PEDOT:PSS-PEO/NBR-PEO bilayer in the same way as the first electrode: new solutions were prepared, cast, and solidified at 50°C by evaporating the water. The resulting trilayer actuators were then placed in a closed annealing chamber and the final heat treatment was carried out at 50°C for 3 h followed by post-curing at 80°C for 1 h under a continuous nitrogen flow. The thicknesses of each PEDOT:PSS-PEO electrode and the NBR-PEO layer obtained were 11 µm and 13 µm, respectively. The trilayer structures were then micro-patterned as microbeams using laser cutting and measured between 5 mm and 6 mm length (L), 1 mm and 1.43 mm wide (w), and 35 ± 1 µm thick (h). To simplify reading, hereinafter the "micro-actuators" will be called "actuators". Before any actuation, the actuator beams were swollen in ionic liquid (IL) –1-ethyl-3-methylimidazolium bis-(trifluoromethylsulfonyl)imide (EMImTFSI)– for 72 h to incorporate in the ECP and ISM, the EMI$^+$ and TFSI$^-$ ions necessary for the actuation process.

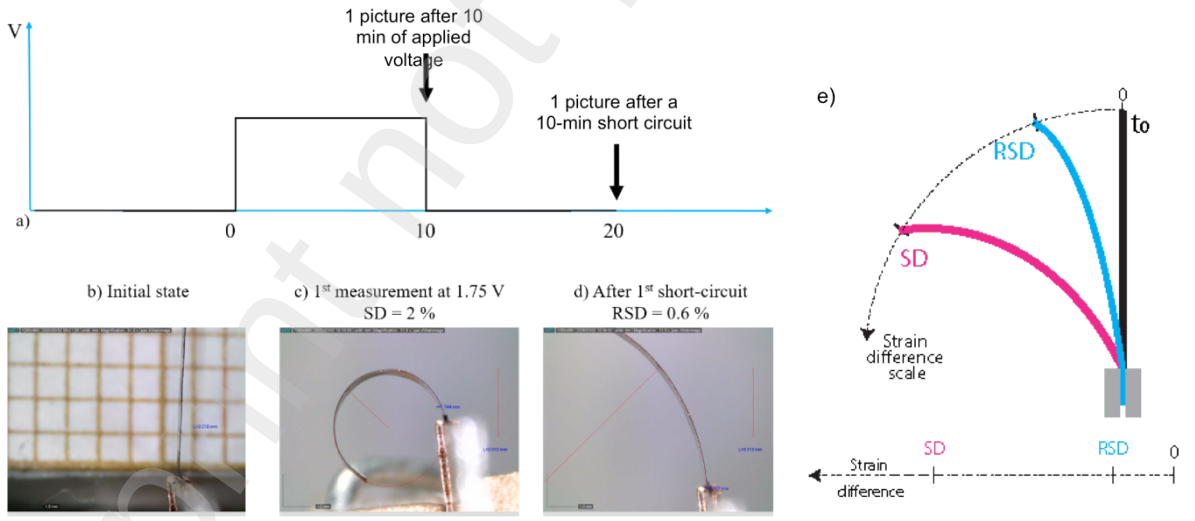

Figure 1: The electromechanical response of the i-EAP was calculated from the initial position (b) to the last position reached by the actuator under an electric voltage (c), and after a short circuit (d). Actuation was characterized using the radius of curvature. To calculate the strain difference (SD) and the residual strain difference (RSD), the actuator strain was assumed to be circular (e).

The actuator was clamped between two copper lines glued to glass slides to allow electrical contact and connect them to the measurement system. During actuation, the actuators were connected to the voltage source (NF Electronic Instruments 1930) and an in-house amplifier to apply a square wave

potential (0.25 – 2.0 V). The experiments were monitored from the side using a Dino Lite AM7000/AD7000 micro camera. Actuator displacement was recorded with the micro camera or a laser LKG 32 Keyence displacement sensor. Due to the large deformations obtained, the strain difference (SD) was calculated from the radius of curvature (Rc) using the micro camera and the following equation: $SD = 100 \times h/Rc$ [33] where h is the thickness of the actuator (Figure 1). The strain difference is an absolute strain which does not consider the initial state of deformation of the actuator as we will see later. The current was measured using a Gamry Potentiostat/Galvanostat ZRA 600+ with the chronoamperometry technique.

2.3. Actuator operation

In Figure 2 we recall the main operating mechanism [34][35][36] of this actuator in air to aid in understanding the mechanisms described in the results and discussion section.

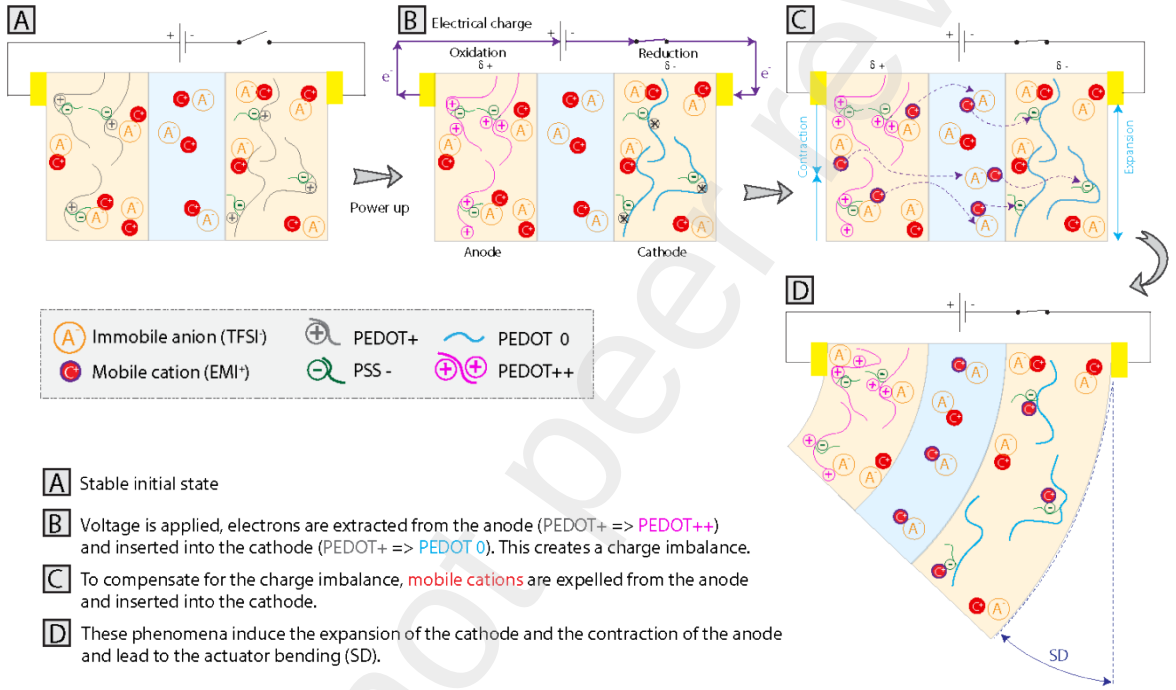

Figure 2: Mechanism of actuation of a trilayer composed of two electronically conducting polymer electrodes and an ion storage membrane saturated with EMITFSI ionic liquid.

Figure 2A: The two electroactive PEDOT:PSS-PEO polymer electrodes are light orange and the ISM is pale green. Although the PEO inside the NBR and the PEDOT:PSS improves charge transport, the ionic conductivity of the ISM, and the electronic conductivity of the PEDOT:PSS [31][37], it is not directly involved in the mechanisms we are going to describe. PEO is not represented schematically for simplification. The incorporation of PEO is also beneficial for the strain performance, most likely related to a higher volumetric charge density but also to a lower Young's modulus than pristine PEDOT:PSS, which facilitates bending. In the electrodes, the oxidized and conducting $PEDOT^+$ and the insulating PSS^- cancel each other out.

Figure 2B: When a voltage is applied across the system, electrons are extracted from the anode side leading to the oxidation of $PEDOT^+$ to $PEDOT^{++}$. Simultaneously, electrons are injected into the cathode side and $PEDOT^+$ is reduced to $PEDOT^0$, which creates a current peak. At this stage, there is an excess of positive charges at the anode and a lack of positive charges at the cathode.

Figure 2C: The electrical balance is restored by the movement of cations: mobile EMI^+ cations are repulsed from the anode to the ISM to prevent an excess of positive charges induced by the oxidation of PEDOT ($PEDOT^+$ to $PEDOT^{++}$), and mobile cations from the ISM are injected into the cathode to offset the charges of PSS^- after the reduction of PEDOT ($PEDOT^+$ to $PEDOT^0$). Indeed, $PEDOT^+$, which has become $PEDOT^0$, can no longer play this role. If the duration of application of the electrical voltage is long enough, it is possible that the entire PEDOT is neutralized, thus rendering this electrode non-conductive. This description is consistent with the mechanism of mobile cations reported previously for PEDOT macro-actuators using EMITFSI as an electrolyte [38]. The ion movement simultaneously leads to an expansion of the cathode and a contraction of the anode.

Figure 2D: This results in the deformation of the actuator. When the voltage is maintained, the cations concentrate more and more in the cathode to counterbalance as much charge as possible. The actuator becomes increasingly deformed for as long as an electrical voltage is applied.

3. Results and discussion

3.1 Time dependence of the strain under a DC voltage and after an open circuit or a short circuit

<u>Strain difference under a DC voltage</u>

The response time is currently a few seconds to several minutes for i-EAP actuators. The characteristics of the electromechanical response of our actuator under a constant voltage are represented in Figure 3a by the SD as a function of time. The actuator was subjected to a voltage of 1.75 V for 100 minutes. Pictures were taken regularly with a micro-camera to measure the radius of curvature and calculate the SD as a function of time. The electromechanical response observed increased monotonically with time and its time dependence was highly nonlinear[39]. The SD increased quickly and reached its maximum after 1150 s, then maintained its deformation relatively well over time. It has been observed experimentally that the electromechanical response of the actuator under a constant voltage comprises three phases: a rapid steady increase, a strain slowdown, and a saturation/relaxation phase. As shown in the zoom in Figure b, the evolution of SD over time can be described by a second order exponential function for the two first phases:

$$SD = SD_{max} - A_1.\left(e^{-t/\tau_1}\right) - A_2.(e^{-t/\tau_2})\#(1)$$

With SD_{max} (SD at t = 1150 s), the amplitude coefficients A_1, A_2, and the time constants τ_1, τ_2.

The first step is very fast with a time constant of 51 s to reach 60 % of the maximum SD value. The second step is slower with a time constant of 372 s to reach 90 % of the maximum SD value. The SD curve then follows a slowly increasing plateau up to 1150 s. The comparison between the SD and the electrical current (blue line) shown in Figure b highlights that the dynamics of the redox process are much faster (about 20 s) than the movement of the ions causing the actuator strain. After 1150 s of actuation, the SD value remains constant for about a further 10 min (600 s), as the uncertainty of the SD measurement is about 5 %.

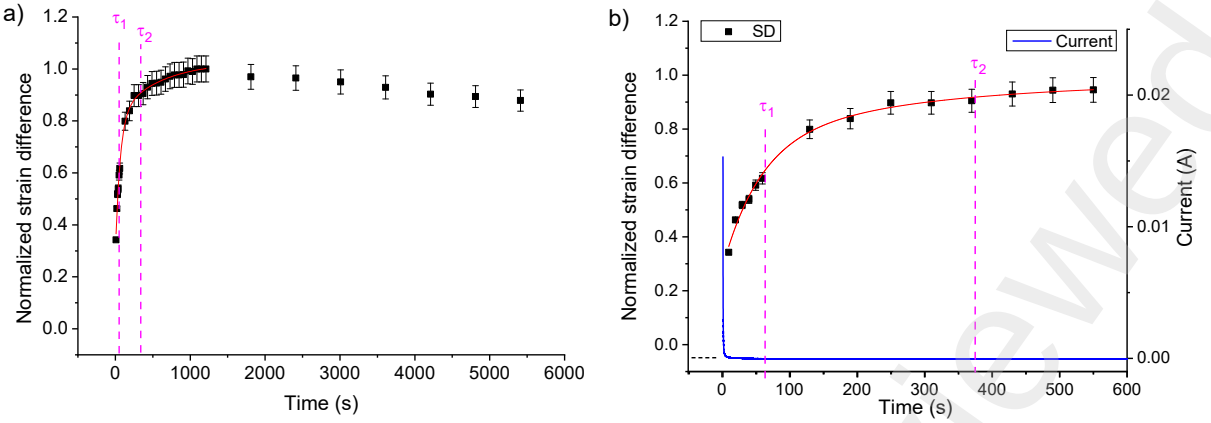

Figure 3: Normalized strain difference as a function of time during a power-up at 1.75 V a) over 2 h and b) zoom over 10 min and the time dependence of the electrical current.

After an hour and a half under an applied voltage, a decrease of around 12 % in SD was observed (Figure a), which is small in comparison with the back-relaxation observed in IPMCs [39]. In the case of these ECP-based actuators, there is no water involved as an ionic liquid is used as the electrolyte. Therefore, the slight relaxation observed under an applied voltage could be due to a slight backflow of ions or a very small leakage current between the electrodes (not observable with our measurement methods). This phenomenon could also be attributed to a small "rebound" effect linked to a period of equilibration between the elastic force of the beam and the force generated by the motion of the ions. This assumption should be verified in future work.

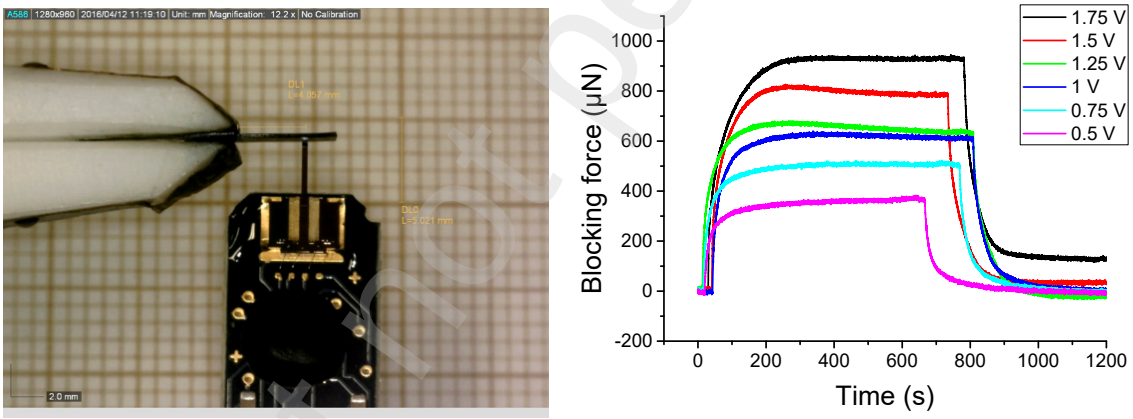

Figure 4: Measurement of the blocking force as a function of time for the different voltages applied

The dynamics of the blocking force under an electrical voltage are quite different from those observed for strain (Figure 4). Indeed, the rise time to reach the maximum strain was about ten minutes (Figure 3b) whereas it was only about thirty seconds (maximum 2 min depending on the voltage applied) for the force. When conducting a blocking force measurement, the force sensor prevents the actuator from moving in the area between the point of embedment and the measurement point. This situation limits the extension of the polymer chains on the cathode side and their contraction on the anode side, thus favoring a more open inter-chain space, and thereby ion mobility, than when the beam bends. This greater freedom of movement of the cations causes the cathode to swell more quickly. Moreover, under an electrical voltage, the force generated by the ECP-based actuator is maintained for at least 10 minutes.

The effect of the inversion of the polarity on the evolution of the strain as a function of time is schematized in Figure 5a and shown in Figure 5b. The strain kinetics of a fresh micro-beam were

measured for an electrical voltage of 1.75 V. A sample was actuated for 40 min (2400 s), then the polarity is reversed for 96 min (5760 s) with no downtime. The SD was determined every second according to the radius of curvature.

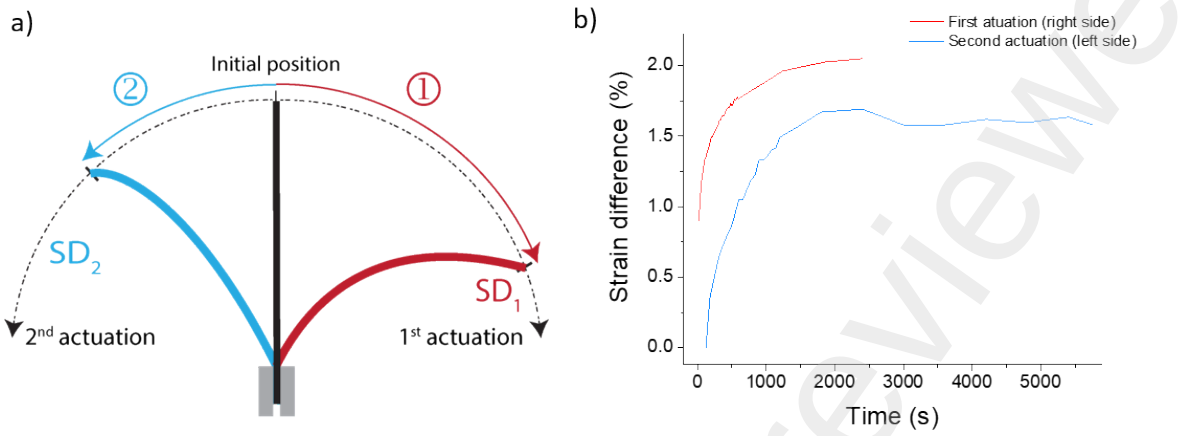

Figure 5: Measurement of SD at 1.75 V as a function of time, first to the right for 2400 s, then to the left for 5760 s, with no short circuit between the two steps and no downtime; a) diagram of the procedure and b) strain kinetics measured for an electrical voltage of 1.75 V for the two directions

It was observed that the actuation speed to reach a constant strain was faster in the initial phase than that obtained after reversing the polarity (Figure 5b). At the end of the first 40 minutes, a SD of 2.0 % was reached. When the voltage was applied in the opposite direction, it took 2 minutes for the actuator to return to its vertical position. The actuator reached a maximum SD of 1.7% after 40 min in this second direction. On the first power-up, 50% of SD_{max} was reached in 30 s, whereas during the reverse actuation this value was reached in 550 s (9 min). This experiment was carried out several times. Depending on the electrical voltage used, the duration of application of this voltage the results may differ, but systematically when the polarization is reversed the strain difference obtained is disturbed by the previous actuation. During the first actuation to the right, the cations, initially homogeneously distributed in the material, are stored for a long time in the left electrode (cathode during this polarisation). When the polarity is reversed, the ions need more time to move to the opposite electrode. It is also possible that some ions remain blocked in or near the left electrode, which would explain the lower SD observed after the polarity was reversed. The first polarity of DC voltage over a long period influences, therefore, the deformation dynamics when the polarity is reversed.

Relaxation in open circuit conditions

The dynamics of relaxation were also studied in open circuit conditions (Figure 6). The actuator was powered up at 1.75 V for 10 min then the circuit was opened. Measurements were carried out using a laser displacement sensor placed at 0.73 mm from the point of embedment of the actuator, the most suitable position to avoid the laser point slipping on the beam as it relaxes. The actuator strain remained constant for almost 2 min then it slowly relaxed. The relaxation was about 0.2 % and 50 % after 30 min and 5 h, respectively. Even after 30 h of rest, the actuator had not returned to its original position. The oxidation and reduction state of the ECP electrodes maintained the deformation without any electrical energy input and despite the beam needing to release its elastic energy. This result shows that when the application concerns moving an object attached to the end of an actuator to keep it in position for example, rather than applying a force on an object, a continuous electrical power supply is not necessary: after opening the circuit, an electrical voltage only needs to be applied to the actuator sequentially. This possibility of operation may be of interest for saving energy in certain applications.

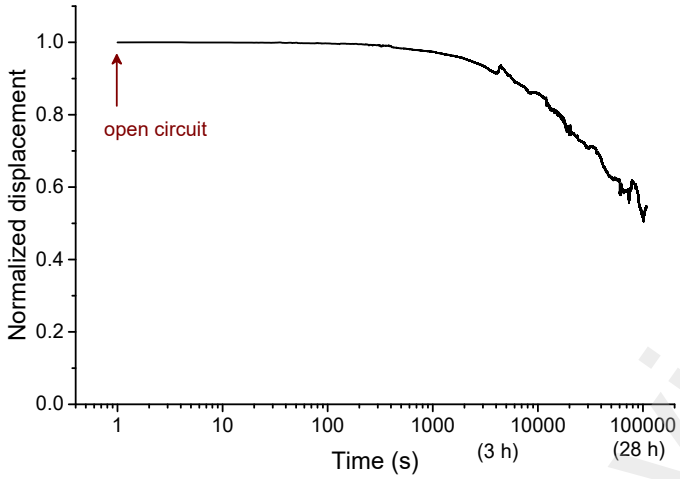

Figure 6: Normalized displacement measured using a laser at 0.73 mm from the point of embedment of the actuator after a 10-min power-up at 1.75 V followed by an open circuit. The displacement was recorded over 30 h.

Relaxation after a short circuit

The time dependence of the actuator after a short circuit was studied and is presented in Figure 7a. The actuator was powered up at 1.75 V for 10 min and then a short circuit was generated.

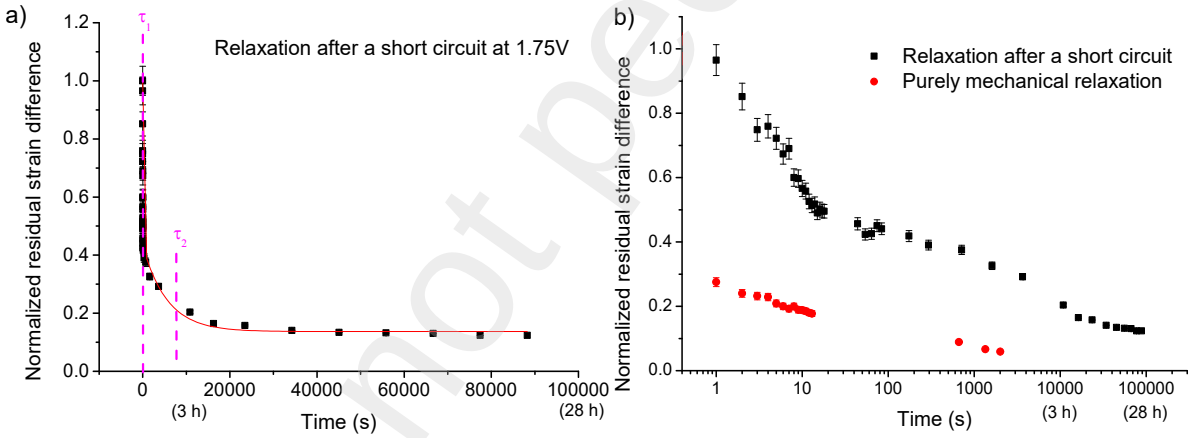

Figure 7: a) Normalized residual strain difference as a function of time after a 10-min power-up at 1.75 V and a short circuit. b) Comparison with purely mechanical relaxation of a same micro beam containing IL: deformation is maintained manually for 10 min then released (the two curves start at y=1).

The dynamics of relaxation during a short circuit can be described by two decreasing exponentials corresponding to a first fast step associated with a time constant τ_1 of 13 s and a second slower step associated with a time constant τ_2 of 7937 s. The relaxation was about 50 % after 26 s and a residual strain difference (RSD) of 0.12 % was still observed after 4 h. Even after 25 h of rest, the actuator had not returned to its original position. An unstable state was established and the actuator only returned to its initial vertical position after a few days.

Relaxation during a short circuit was then compared with purely mechanical relaxation of the actuator (Figure 7b). To reproduce the strain but without a power supply, the actuator was saturated with IL and then bent around a cylindrical rod. This strain was maintained for 10 minutes before removing the blocking system. After approximately 2000 s, the RSD measured was null, indicating that the actuator

had returned to its initial position. The dynamics of purely mechanical relaxation can be described by three decreasing exponentials: an extremely fast first step associated with a time constant τ_1 of only 0.3 s, a second intermediate step with a time constant τ_2 of 5 s, and a final slower step with a time constant τ_3 of 524 s. This purely mechanical relaxation is much faster than relaxation during a short circuit, indicating that ionic and electrical processes are also involved.

As explained in Figure , when power is applied the actuator bends because of the movement of the cations towards the cathode. This strain goes against the rest position of the polymer chains which are thus stretched on one side and compressed on the other. Therefore, when a short circuit is generated, a combination of at least two phenomena is considered: (i) the mechanical relaxation of the beam and (ii) the backflow of cations.

i) When the short circuit is generated, the beam releases the mechanical energy resulting from the viscoelasticity of the material. The polymer chains extended on one side and compressed on the other seek to return to their original position and dimensions. Consequently, cation expulsion and thereby beam relaxation are a combination of mechanical and electrical effects. The comparison of purely mechanical relaxation and relaxation following an electrical power-up and a short circuit (Figure 7b) shows that cation backflow slows down mechanical relaxation. During the first relaxation step under a short circuit, mechanical relaxation appears to be the main contributor whereas the cations partly trapped slow down the overall process. During the last step, however, mechanical relaxation may still occur but it is more the cation backflow that promotes actuator relaxation.

ii) The short circuit enables electrons to flow between the ECP electrodes thus inducing a discharge peak of electrical current. This electrical charge causes the electrons to recombine on the polymer chains and PEDOT tends recover its initial oxidation state, releasing the cations that played the role of charge compensators for the PSS-. Cations are thus expelled from the cathode and attracted by the anode. This backflow of cations changes the contraction/extension state of the ECP electrodes which tend to return to their previous dimensions. This phenomenon leads to beam relaxation; it is, however, rather slow in comparison with pure mechanical relaxation. When the cations are charge compensators for PSS-, they are located in interstitial positions in a dense matrix of polymer chains. They are, therefore, slightly trapped due to the fast mechanical return of the actuator, thus limiting their mobility and lowering the backflow rate for as long as a reverse electrical voltage is applied.

3.2 Strain and residual strain as a function of decreasing DC voltage

To study this aspect in more detail, additional measurements were performed. In the following experiments, actuators were submitted to actuation for 10 min at a chosen voltage, followed by a short circuit for 10 min. The SD and RSD were determined from the position of the actuator after 10 min of actuation and after a 10 min short circuit, respectively. The calculation of the strain difference amplitude (SDa) under an applied voltage and the residual strain difference amplitude (RSDa) is explained in Figure 8.

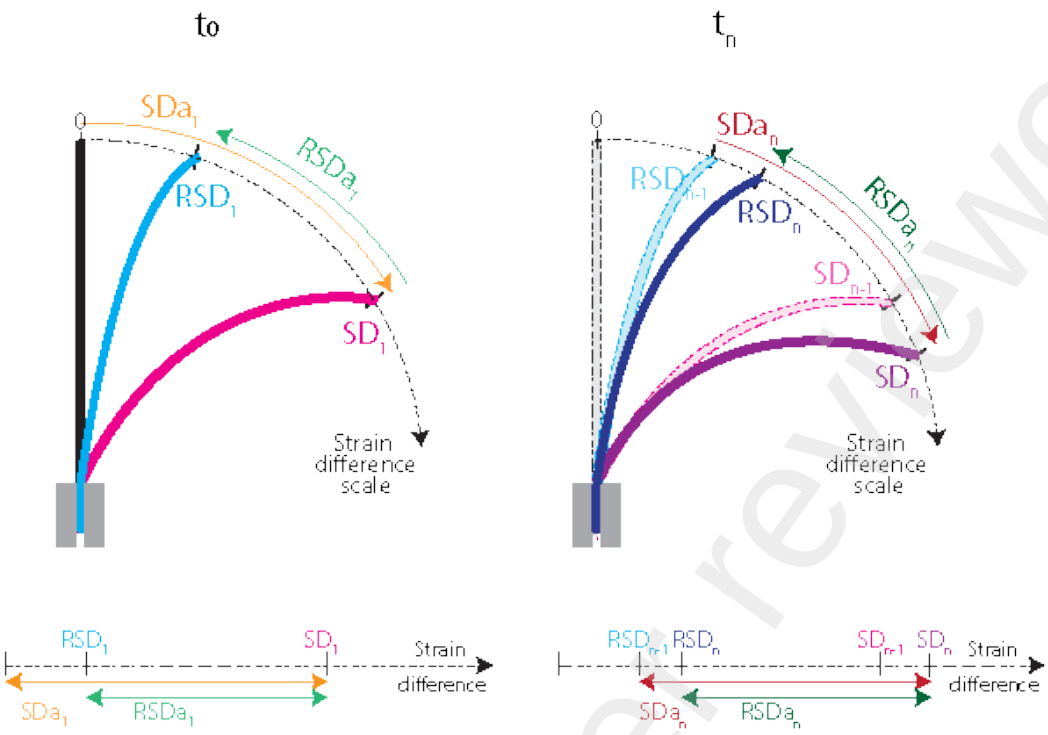

Figure 8: The SD and RSD were determined from the position of the actuator after 10 min of actuation and after a 10 min short circuit, respectively. The strain difference amplitude under an applied voltage (SDa) is the amplitude between the initial position of the beam and the final position after applying a voltage for 10 min. The residual strain difference amplitude (RSDa), i.e. the amplitude of movement of the actuator during a short circuit, is the amplitude between the last position under an applied voltage and the position after a 10 min short circuit. SDa and RSDa can be calculated according to equations $SDa_n = SD_n - RSD_{n-1}$ *and* $RSDa_n = SD_n - RSD_n$*, respectively, where n is the number of actuations.*

An initial series of actuations at voltages decreasing in increments of 0.25 V from 1.75 V to 0.5 V was conducted on a fresh actuator that had never been used before. In this case, the initial ion distribution inside the actuator was assumed to be homogenous. Then, after 20 h of rest under a short circuit, a second identical series of actuations was conducted on the same sample (Figure 9a). During this time, the ions could flow back and tended to recover their initial homogenous distribution.

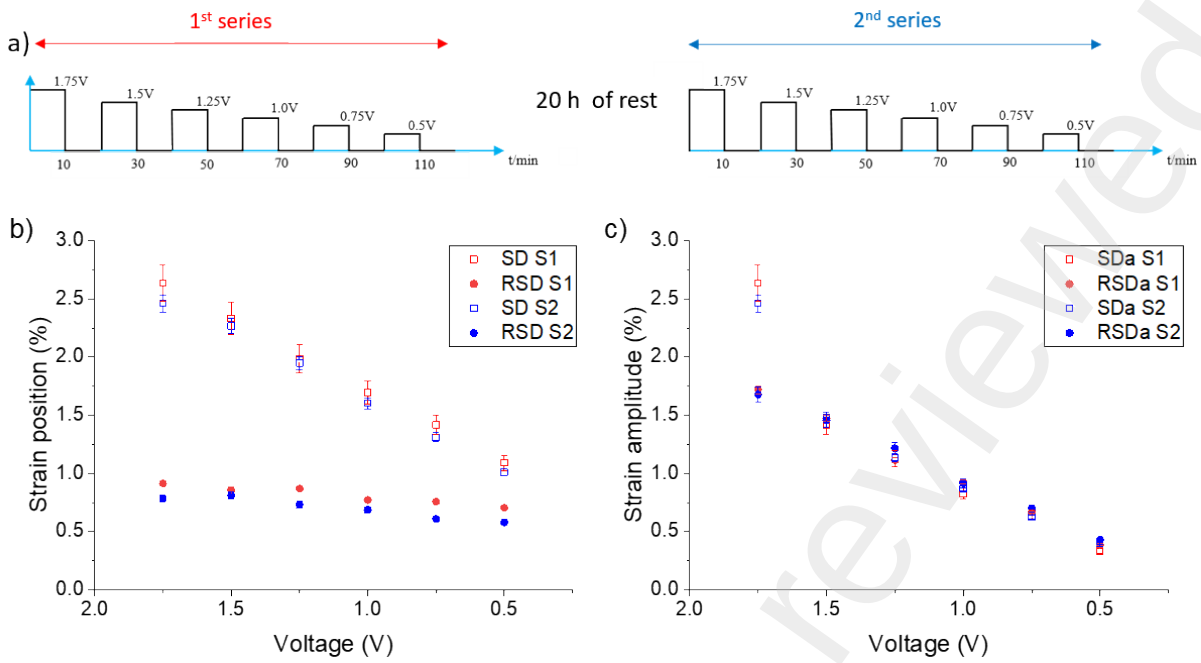

Figure 9: a) Chronovoltamogram of the experiment, b) strain and residual strain differences as a function of the applied voltage related to the actuator position, and c) the strain difference amplitude under an applied voltage and the residual strain difference amplitude.

The SD and RSD corresponding to the position reached by the actuator during both series are shown in Figure 9b. The SDa and RSDa corresponding to the amplitude of movement of the actuator during both series are shown in Figure c. The main results are as follows:

- The SD decreased linearly with the applied voltage (Figure 9b). After 10 min, the final position reached by the actuator, i.e. the quantity of cations that could be mobilized, was proportional to the DC voltage applied. Therefore, ion mobility and the electrical processes are correlated up to 1.75 V, as expected. However, we noticed that leaving the actuator under an electrical voltage beyond 1.75 V for a long time damages the actuator.
- The RSD values are not null (Figure 9b), which means that the actuator did not return to its initial vertical position. As mentioned previously (Figure 7b), the complete relaxation of an actuator under a short circuit after 10 min of actuation at 1.75 V occurs only after a few days. Therefore, a short circuit of 10 min is insufficient for the cations, concentrated at the cathode, to flow back thus resulting in the residual strain measured. The RSD decreased slightly with decreasing voltage but remained between 0.70 % and 0.91 % for the first series and between 0.58 % and 0.78 % for the second series. Consequently, starting with the application of a high electrical voltage blocks the cations preventing the cathode from returning to its non-elongated position. Then, whatever the lower electrical voltage applied to the actuator, the proportion of cations that can no longer escape from the polymer chains of the PEDOT:PPS cathode remains roughly the same.
- The SD and RSD of the positions reached by the actuator during the 2nd series were very close but slightly lower than that of the 1st series, which shows the reproducibility of the process (Figure 9b) after being exposed to short-circuit during 20h.
- For both series (except for the first SDa measured at 1.75 V), the amplitudes of the strain difference and the residual strain difference can be superimposed. Therefore, for a given voltage, the same fraction of cations moved when the voltage was applied as during the short circuit (Figure 9c).

- For each series, the SDa value measured for the first actuation (at 1.75 V) was higher and is not aligned with the SDa obtained for lower voltages (1.5 to 0.5 V) (Figure c). This indicates that when the cation distribution is initially homogeneous or has regained a certain homogeneity in the actuator due to resting the material, the dynamics of movement and thereby the strain amplitude, are amplified. A rest time of 20 h between the two series is almost sufficient to regenerate the initial properties of the actuator.
- Moreover, if actuation at 1.75 V is conducted immediately after the decreasing series, the SDa measured is well aligned with the previous ones at lower voltages (supplementary materials, Figure S1).

As the ionic and electrical processes are correlated, a similar experiment was conducted on the currents and the quantities of switched charges. A series of actuations at voltages decreasing in increments of 0.25 V from 1.75 V to 0.5 V was performed on a new sample.

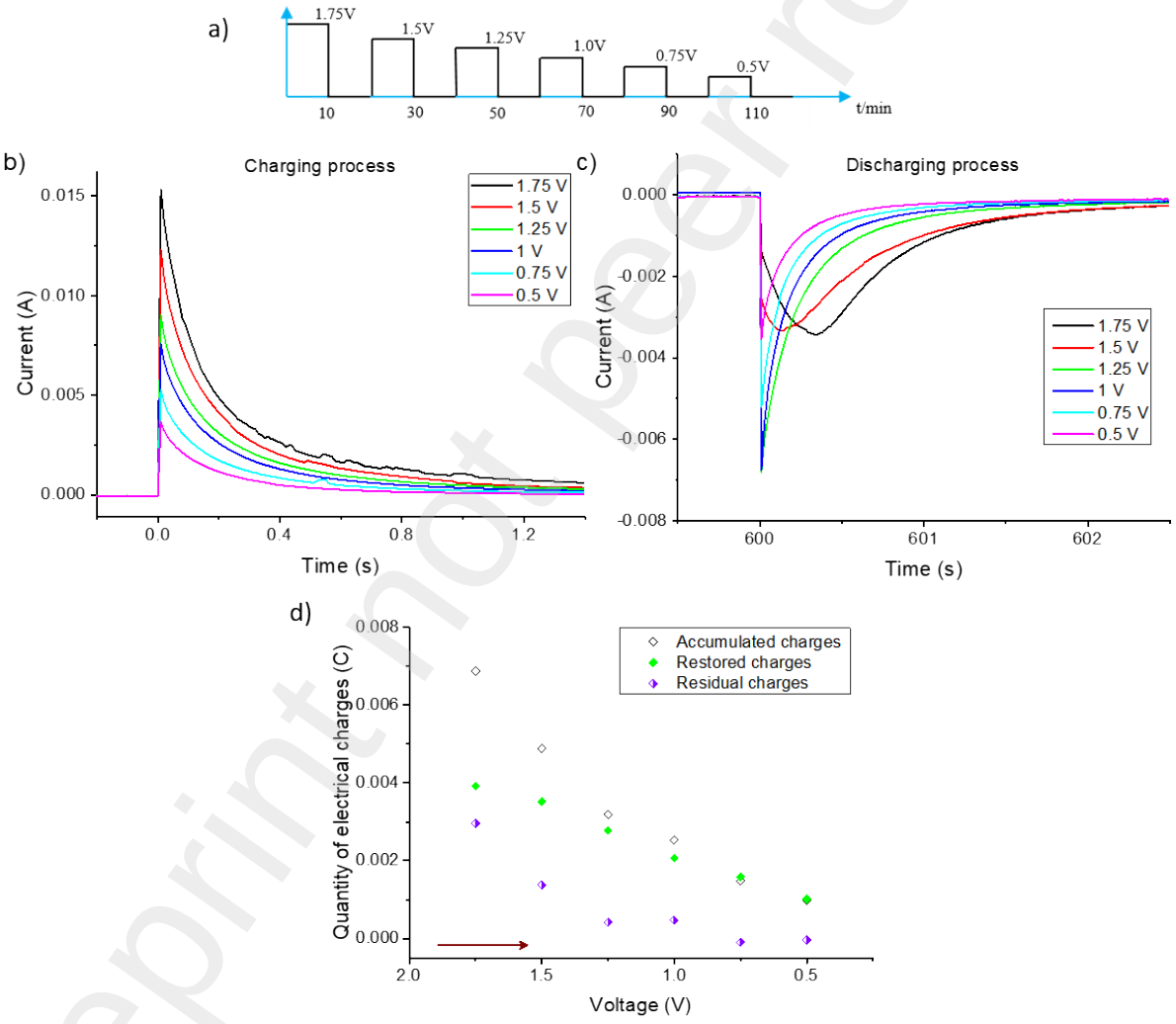

Figure 10: a) Chronovoltamogram of the experiment. Currents measured with zoom on the transient regime for different voltage levels: charging (b) and discharging (c). d) Evolution as a function of the applied voltage of the amount of charge stored, restored, and not restored.

The charging (Figure 10a) and discharging currents (Figure 10b) measured during the oxidation/reduction processes are presented. During the charging process, the current reaches a maximum value and falls back to zero because the duration is sufficiently long. During the charging process, the aspect of the peak current is the same for all the voltages applied, and its height decreases when the applied voltage decreases.

The amount of charges after 10 min of applied voltage and the charges that appear during the short circuit were calculated by integrating the current peaks. The difference between both represents the amount of "not restored charges" (Figure 10d). Not restored charges appear with applied voltages of 1.75 V and 1.5 V (Figure 10d). The flattening of the current peak during the short circuit is unlike that obtained when switching on at 1.75 V and then at 1.5 V (Figure 10b). This result demonstrates that some of the oxidation sites are no longer available for reduction: The small potentials only partially reduce the PEDOT, which weakens its electronic conductivity but does not prevent its subsequent re-oxidation. For the highest voltages combined with long times of electrical voltage applied, the PEDOT is more deeply reduced and makes it quasi insulating and does not contribute its re-oxidation and the release of charge equivalent to those obtained during of the reduction phase. Moreover, some of the cations do not flow back from the cathode when the short circuit is generated thus preventing also the reduction of certain sites. This is directly related to the occurrence of a RSD, as observed in Figure . Moreover, for these two voltages applied, the discharging current peaks are lower and larger than those obtained during charging, indicating a very slow discharge process which is no longer comparable to a simple RC circuit (Figure 10d). The amount of not restored charges is near zero when the applied voltage is below 1.25 V indicating that the amount of moving charges is the same as the charges restored during the short circuit for these voltages applied. This means that for lower voltages and after blocking some sites, charges that may have accumulated are fully restored. In this case, the RSD is maintained due to the initial amount of not restored charges caused by the applied voltages of 1.75 V and 1.5 V. As these non-linearities only appear for higher voltages and the voltages are applied to the falling edge, one might wonder what would happen if the voltage was applied to the rising edge.

3.2 Strain and residual strain as a function of increasing DC voltage

For the next experiment, a series of actuations at voltages increasing in increments of 0.25 V from 0.5 V to 1.75 V was performed on a fresh sample (Figure a). In this case, both the deformation and the electrical results are discussed simultaneously and chronologically. All the actuations were performed in the same direction. The evolution of SD and RSD referring to the position of the beam and SDa and RSDa referring to the amplitude of movement of the actuator as a function of time are reported in Figure b and 11c, respectively. The raw current measured at room temperature is presented in the supplementary materials (Figure S2) for the charging and discharging processes. The calculated resistance and the amount of accumulated, restored, and not restored charges are reported as a function of time in Figure d) and e), respectively.

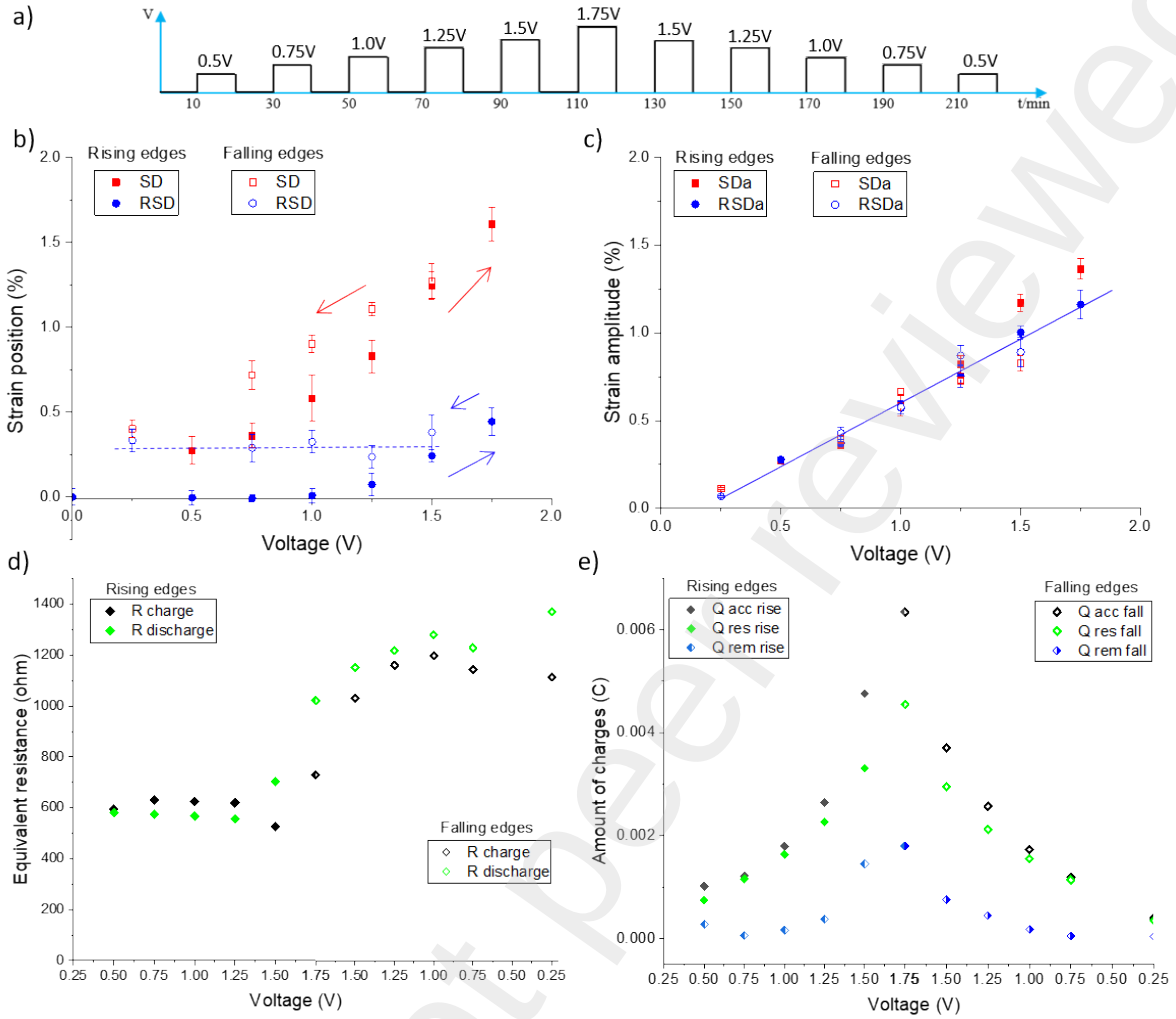

Figure 11: a) Chronovoltamogram of the experiment. Evolution as a function of the applied voltage of b) strain position (SD and RSD), c) strain amplitude (SDa, RSDa), d) equivalent resistance of charge (Rc) and discharge (Rd) processes, and e) electrical charges (accumulated (Q acc), restored (Q res) and not restored (Q rem)).

Before actuation, the actuator was fresh and the cations were assumed to be homogeneously distributed. For actuations from 0.5 V to 1.0 V, the position reached by the actuator under an applied voltage (SD) increased moderately and the RSD after a 10-min short circuit was null (Figure 11b). Therefore, the amplitudes of movement were the same (SDa and RSDa): the beam returned to its initial position and the amplitude increased with the applied voltage (Figure 11c). The amount of charges accumulated and restored was the same for a given voltage and increased linearly with the applied voltage (Figure 11e). There were no residual charges and the equivalent resistance was similar in the charging and discharging processes (Figure 11d). For voltages up to 1.0 V, there was no blocking effect and both the ionic and electrical processes were enhanced and reversible when the voltage increased.

From 1.25 V, the blocking effect began and increased with the voltage as the RSD was no longer null. The position and amplitude of the actuator under an applied voltage (SD and SDa respectively) increased linearly. The actuator no longer returned to its initial position (Figure 11b). Similarly, the amount of accumulated charges increased more than the amount of restored charges resulting in the appearance of residual charges, of which the amount increased as the voltage increased. Finally, the

resistance during the charging and discharging process remained stable at around 600 Ω down to 1.5 V but increased from 1.5 V and became higher for the discharging process than the charging process. This is consistent with the lower amount of restored charges compared to the amount of accumulated charges. Figure 11c shows that the RSDa is still proportional to the voltage whereas the SDa increases more quickly from 1.25 V compared to RSDa indicating a slight change in the physical phenomena involved in the deformation of the material; this is confirmed by an oxidation process yielding proportionally a lot more electrons (Figure 11e).

In the falling edge, the SD decreased with the applied voltage and is not superimposed with the data acquired in the rising edge: the global deformation in the falling edge is greater due to the presence of an initial non-zero RSD (Figure 11b) maintained at around 0.25 % whatever the decreasing voltage value. This RSD that remains constant with a decreasing applied voltage confirms again that after the application of a high electrical voltage (1.75 V) some of the cations and sites for oxidation remain blocked preventing the material from returning to the initial position it was in before an electrical voltage was applied. Despite this, the SDa and RSDa remained proportional to the applied voltage. When cations remain blocked, charges during the oxidation/reduction processes and the current are reduced causing an increase in the resistance of the actuator, as can be seen in Figure 11d. Below 1.25 V, the accumulated and restored charges are very similar because there are no additional charge blockages for these voltages. Moreover, the amount of accumulated and restored charges is close to the data acquired in the rising edge step.

The last experiment was conducted at 1.75 V and 1.0 V to investigate if the intensity of the blocking effect increases when multiple actuations are performed at the same voltage. The results of the strain position (SD and RSD), strain amplitude (SDa, RSDa), electrical charge (accumulated, restored, and blocking), and resistance (charging and discharging processes) are reported in Figure 12a, b, c, and d, respectively.

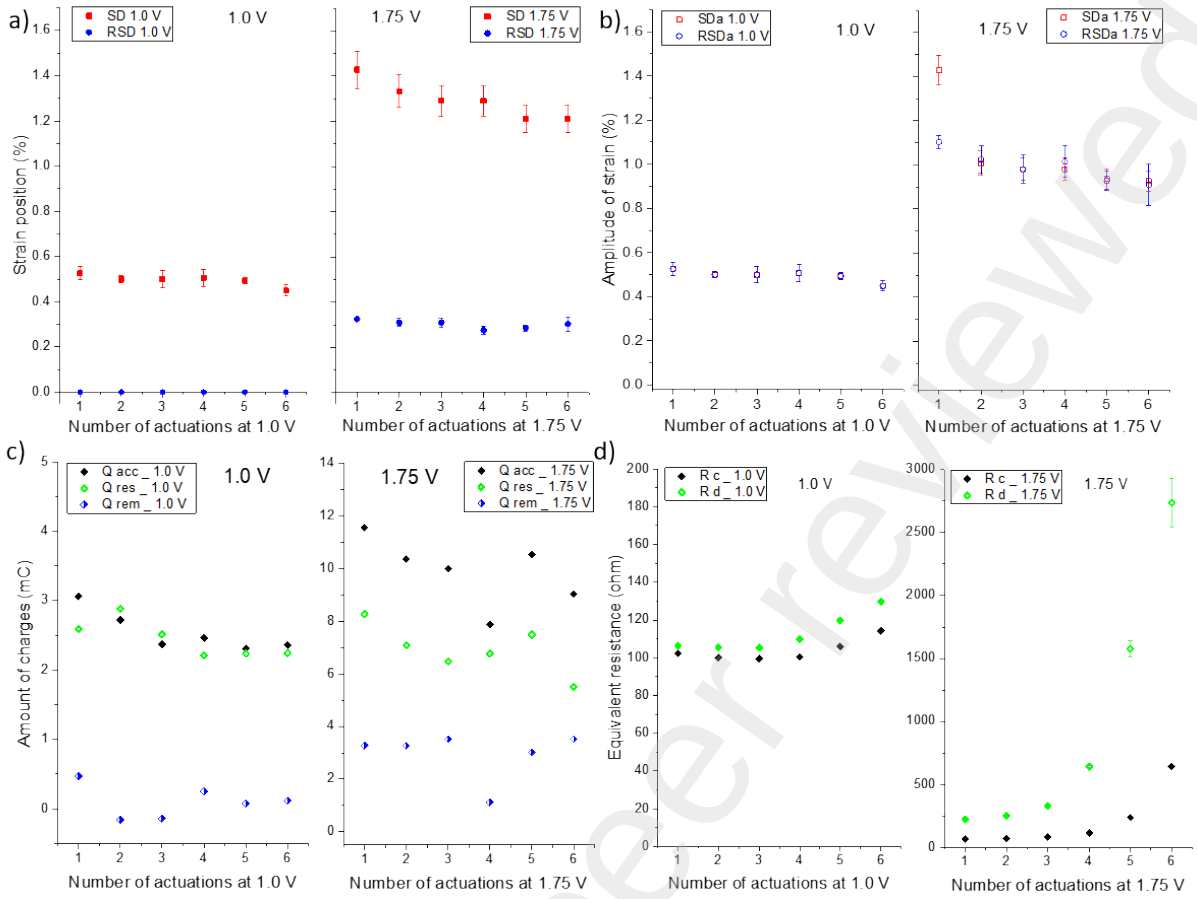

Figure 12: Evolution as a function of the number of actuations of a) strain position (SD and RSD), b) strain amplitude (SDa, RSDa), c) electrical charge (accumulated (Q acc), restored (Q res) and residual (Q rem), and d) equivalent resistance of charging (Rc) and discharging (Rd) processes.

At 1.0 V, the SD was relatively constant as the number of actuations increased and the RSD was null (Figure 12a). At 1.75 V, the SD was higher than at 1.0 V and decreased slightly with the multiplication of actuations. The RSD was about 0.33 % and remained constant. Therefore, for each series, the SDa and RSDa were superimposed at a given voltage, except for the first actuation at 1.75 V for which the amplitude was higher (Figure 12b).

Concerning the movement of the electrical charges (Figure 12c), all the accumulated charges were restored at 1.0 V whereas at 1.75 V charges were not restored and their amount remained quite constant even when additional actuations were performed. Finally, the resistance (Figure 12d) was constant and equal for both the charging and discharging processes at 1.0 V. However, at 1.75 V, Rc was always lower than Rd, especially after 4 actuations. They increased slightly during the first three actuations and then increased nine-fold between the third and sixth actuations.

Therefore, there was no blocking effect at 1.0 V, even with multiple actuations. However, at 1.75 V the blocking effect occurred with the first actuation but was not enhanced by additional actuations. The amount of non-blocking charges and the degree of RSD were constant but the resistance increased and the amplitude of strain difference decreased. This suggests actuator fatigue when operating for long durations (a total of 60 minutes) at high voltages such as 1.75 V.

- *Proposed mechanism*

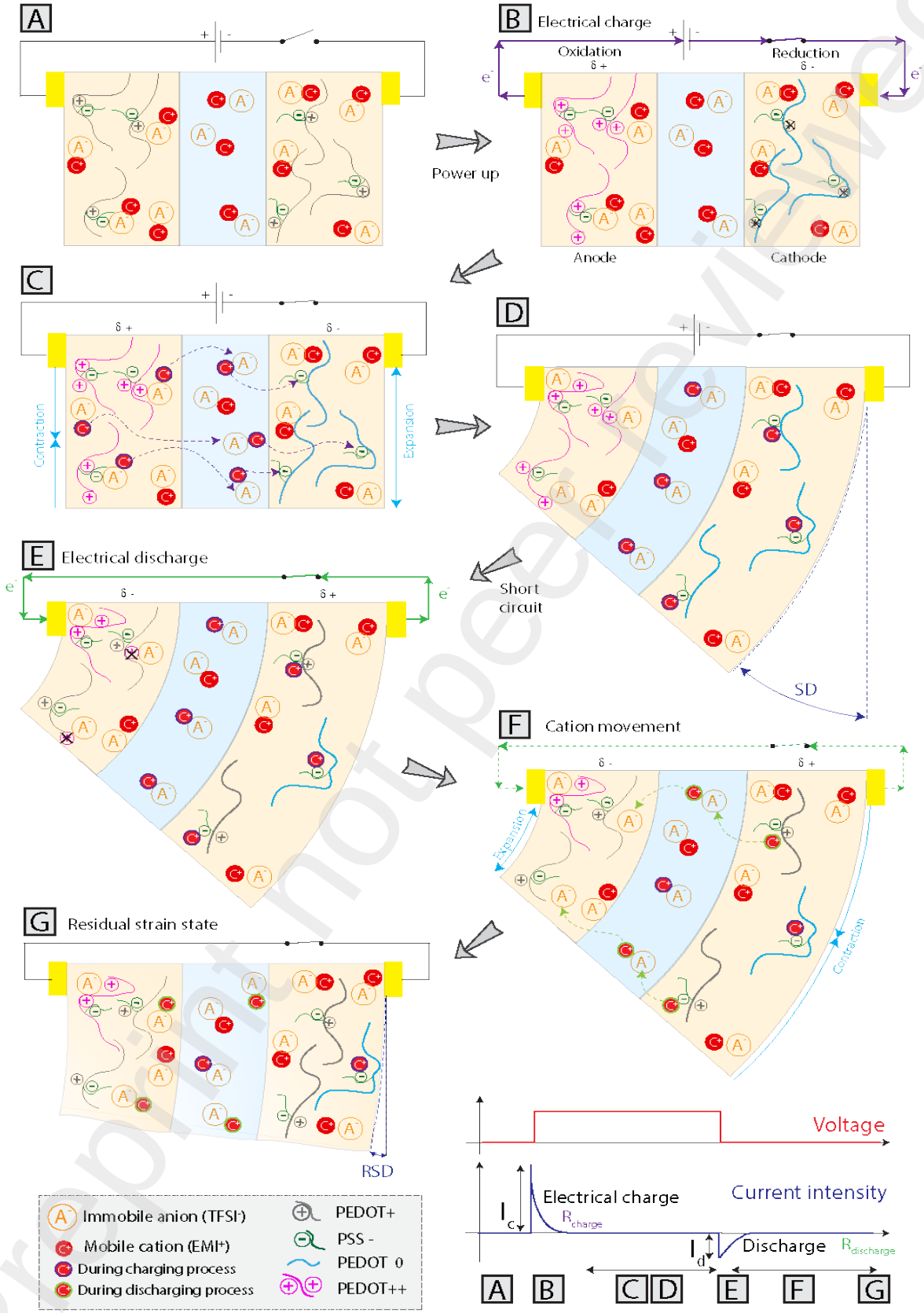

Figure 13: Proposed mechanism to illustrate the memory effect induced by cation blocking.

To illustrate the processes involved with DC voltages (10 min) of 1.25 V and above, the following mechanistic scheme is proposed (Figure). The first part of the actuation mechanism, steps A to D, is the same as described in Figure 2. We will therefore describe from E. In this phase where a short circuit is caused, it is no longer possible to speak of anode and cathode which will be replace by left electrode and right electrode respectively.

E: When a short circuit is generated, the oxidized PEDOT (i.e. $PEDOT^{++}$) at the left electrode accepts an electron flow to become $PEDOT^{+}$ again. At the same time, by releasing these electrons at the right electrode, $PEDOT^{0}$ becomes $PEDOT^{+}$. However, contrary to a classical capacitor for which the charging and discharging phenomena are equivalent, the presence of blocked sites for oxidation and blocked cations at the right electrode slows down the departure of electrons, especially as there is no energy input. Thus, the amplitude of the discharge current peak (Id) is lower and the associated discharge resistance (Rd) is higher. The discharge peak is larger because the process is slower than the charging process.

F: The system is again in disequilibrium and is counterbalanced by the movement of cations. Excess cations flow from the right electrode to the ISM and the positive charge deficiency at the electrode left attracts cations from the ISM. As the cations flow back from the right electrode, they allow the oxidation of $PEDOT^{0}$ chains to $PEDOT^{+}$. The electrical and ionic processes are thus concomitant and interdependent. The backflow of cations progressively leads to the expansion of the electrode left and the compression of the electrode right. The beam straightens and gradually tends towards its initial position.

G: Nevertheless, some cations are strongly "associated" with PSS^{-}, either electrically or through a form of blocking due to the polymer chains weakening cation mobility. These cations will therefore move less easily (free themselves), especially as in this situation no additional electrical energy is supplied to help them do so. These cations continue to act as charge compensators for PSS^{-} and prevent locally $PEDOT^{0}$ from reconverting to $PEDOT^{+}$ at the right electrode. Therefore, some of the charges accumulated during the charging process are not restored during the discharging process, thereby constituting residual charges and leading to a non-null RSD.

CONCLUSION

Some micro-robotics devices require DC actuation to maintain a given position for a few minutes. The use of conducting polymer-based actuators is increasingly considered, particularly in the medical field where low electrical voltages are required. The work presented here highlights certain aspects regarding the operation of conducting polymer-based actuators subjected to a DC voltage for several minutes so that the data can be used subsequently for controlling the position of a micro-object for example. The results have shown that the actuators described in this article maintain a relatively fixed position under an electrical voltage with no relaxation effect, contrary to what is commonly observed in IPMCs. The position can also be maintained in air with an open circuit for several minutes. A short circuit causes the rapid relaxation of the actuator, which is the competition between mechanical relaxation and ion backflow allowing the deformation of the material. Mechanical relaxation is slowed down by the backflow of ions, all the more when the electrical voltage initially applied is high (1.75V). If an electrical voltage greater than 1.25V is applied to the actuator for several minutes then some of the ions remain blocked at an electrode and are no longer available to participate in the actuation of

the material. This situation results in an RSD, a loss of switchable electrical charges, and finally induces a position in space of the actuator which may depend on the electrical activation the actuator was subjected to previously. This fact will be of great importance for developing technological applications using conducting polymer actuators.

ACKNOWLEDGMENTS

This work was supported by the H2020 project TWINNIMS (Grant agreement 857263) and the French Government through the National Research Agency (ANR) with the ROBOCOP (ANR-19-CE19-0026), PIA EQUIPEX LEAF (ANR-11-EQPX-0025) projects. The work was also in part funded by the French 'Renatech' network and by the Région Hauts-de-France.

REFERENCES

[1] M. Shahinpoor, Ionic polymer-conductor composites as biomimetic sensors, robotic actuators and artificial muscles - A review, Electrochim. Acta. 48 (2003) 2343–2353. https://doi.org/10.1016/S0013-4686(03)00224-X.

[2] A. Maziz, C. Plesse, C. Soyer, C. Chevrot, D. Teyssié, E. Cattan, F. Vidal, Demonstrating kHz frequency actuation for conducting polymer microactuators, Adv. Funct. Mater. 24 (2014) 4851–4859. https://doi.org/10.1002/adfm.201400373.

[3] M. Shahinpoor, K.J. Kim, Ionic Polymer Metal Composites (IMPCs): Smart Multi-Functional Materials and Artificial Muscles, 2015.

[4] I.S. Park, S.M. Kim, D. Pugal, L. Huang, S.W. Tam-Chang, K.J. Kim, Visualization of the cation migration in ionic polymer-metal composite under an electric field, Appl. Phys. Lett. 96 (2010) 043301. https://doi.org/10.1063/1.3293290.

[5] K. Asaka, K. Oguro, Y. Nishimura, M. Mizuhata, H. Takenaka, Bending of Polyelectrolyte Membrane-Platinum Composites by Electric Stimuli I. Response Characteristics to Various Waveforms, Polym. J. 27 (1995) 436–440. https://doi.org/10.1295/polymj.27.436.

[6] S. Nemat-Nasser, Y. Wu, Comparative experimental study of ionic polymer-metal composites with different backbone ionomers and in various cation forms, J. Appl. Phys. 93 (2003) 5255–5267. https://doi.org/10.1063/1.1563300.

[7] S. Nemat-Nasser, S. Zamani, Y. Tor, Effect of solvents on the chemical and physical properties of ionic polymer-metal composites, J. Appl. Phys. 99 (2006). https://doi.org/10.1063/1.2194127.

[8] Z. Zhu, L. Chang, K. Takagi, Y. Wang, H. Chen, D. Li, Water content criterion for relaxation deformation of Nafion based ionic polymer metal composites doped with alkali cations, Appl. Phys. Lett. 105 (2014) 1–4. https://doi.org/10.1063/1.4892636.

[9] S. Nemat-Nasser, Y. Wu, Tailoring the actuation of ionic polymer-metal composites, Smart Mater. Struct. 15 (2006) 909–923. https://doi.org/10.1088/0964-1726/15/4/003.

[10] S. Nemat-Nasser, S. Zamani, Modeling of electrochemomechanical response of ionic polymer-metal composites with various solvents, J. Appl. Phys. 100 (2006). https://doi.org/10.1063/1.2221505.

[11] Y. Bar-Cohen, X. Bao, S. Sherrit, S.-S. Lih, Characterization of the electromechanical properties of ionomeric polymer-metal composite (IPMC), Smart Struct. Mater. 2002 Electroact. Polym. Actuators Devices. 4695 (2002) 286–293. https://doi.org/10.1117/12.475173.

[12] M. Porfiri, A. Leronni, L. Bardella, An alternative explanation of back-relaxation in ionic polymer metal composites, Extrem. Mech. Lett. 13 (2017) 78–83. https://doi.org/10.1016/j.eml.2017.01.009.

[13] V. Vunder, A. Punning, A. Aabloo, Mechanical interpretation of back-relaxation of ionic electroactive polymer actuators, Smart Mater. Struct. 21 (2012). https://doi.org/10.1088/0964-1726/21/11/115023.

[14] Y. Liu, S. Liu, J. Lin, D. Wang, V. Jain, R. Montazami, J.R. Heflin, J. Li, L. Madsen, Q.M. Zhang, Ion transport and storage of ionic liquids in ionic polymer conductor network composites, Appl. Phys. Lett. 96 (2010) 15–18. https://doi.org/10.1063/1.3432664.

[15] L.A. Hirano, L.W. Acerbi, K. Kikuchi, S. Tsuchitani, C.H. Scuracchio, Study of the influence of the hydration level on the electromechanical behavior of nafion based ionomeric polymer-metal composites actuators, Mater. Res. 18 (2015) 154–158. https://doi.org/10.1590/1516-1439.353214.

[16] M. Annabestani, M. Maymandi-Nejad, N. Naghavi, Restraining IPMC Back Relaxation in Large Bending Displacements: Applying Non-Feedback Local Gaussian Disturbance by Patterned Electrodes, IEEE Trans. Electron Devices. 63 (2016) 1689–1695. https://doi.org/10.1109/TED.2016.2530144.

[17] M.J. Fleming, K.J. Kim, K.K. Leang, Mitigating IPMC back relaxation through feedforward and feedback control of patterned electrodes, Smart Mater. Struct. 21 (2012). https://doi.org/10.1088/0964-1726/21/8/085002.

[18] M. Shahinpoor, K.J. Kim, Ionic polymer-metal composites: III. Modeling and simulation as biomimetic sensors, actuators, transducers, and artificial muscles, Smart Mater. Struct. 13 (2004) 1362–1388. https://doi.org/10.1088/0964-1726/13/6/009.

[19] R.H. Baughman, L.W. Shacklette, R.L. Elsenbaumer, E.J. Plichta, C. Becht, Micro Electromechanical Actuators Based on Conducting Polymers BT - Molecular Electronics: Materials and Methods, in: P.I. Lazarev (Ed.), Springer Netherlands, Dordrecht, 1991: pp. 267–289. https://doi.org/10.1007/978-94-011-3392-0_27.

[20] A.S. Hutchison, T.W. Lewis, S.E. Moulton, G.M. Spinks, G.G. Wallace, Development of polypyrrole-based electromechanical actuators, Synth. Met. 113 (2000) 121–127. https://doi.org/10.1016/S0379-6779(00)00190-9.

[21] A. Mazzoldi, A. Della Santa, D. De Rossi, Conducting Polymer Actuators: Properties and Modeling BT - Polymer Sensors and Actuators, in: Y. Osada, D.E. De Rossi (Eds.), Springer Berlin Heidelberg, Berlin, Heidelberg, 2000: pp. 207–244. https://doi.org/10.1007/978-3-662-04068-3_7.

[22] J.D. Madden, P.G. Madden, I.W. Hunter, Polypyrrole actuators: modeling and performance, Smart Struct. Mater. 2001 Electroact. Polym. Actuators Devices. 4329 (2001) 72. https://doi.org/10.1117/12.432688.

[23] T.F. Otero, Artifical Muscles, Electrodissolution and Redox Processes in Conducting Polymers, in: Handb. Org. Conduct. Mol. Polym., 1997: pp. 517–594.

[24] C. Odin, M. Nechtschein, Memory effect in conducting polymers: Electrochemical and ESR studies on polyaniline, Synth. Met. 43 (1991) 2943–2946. https://doi.org/10.1016/0379-

6779(91)91212-S.

[25] H. Grande, T.F. Otero, Conformational movements explain logarithmic relaxation in conducting polymers, Electrochim. Acta. 44 (1999) 1893–1900. https://doi.org/10.1016/S0013-4686(98)00298-9.

[26] H. Grande, T.F. Otero, Intrinsic asymmetry, hysteresis, and conformational relaxation during redox switching in polypyrrole: A coulovoltametric study, J. Phys. Chem. B. 102 (1998) 7535–7540. https://doi.org/10.1021/jp9815356.

[27] T.F. Otero, H.J. Grande, J. Rodríguez, Reinterpretation of polypyrrole electrochemistry after consideration of conformational relaxation processes, J. Phys. Chem. B. (1997). https://doi.org/10.1021/jp9630277.

[28] M.A. Vorotyntsev, M. Skompska, E. Pousson, J. Goux, C. Moise, Memory effects in functionalized conducting polymer films: Titanocene derivatized polypyrrole in contact with THF solutions, J. Electroanal. Chem. 552 (2003) 307–317. https://doi.org/10.1016/S0022-0728(03)00038-X.

[29] T. Sendai, H. Suematsu, K. Kaneto, Anisotropic strain and memory effect in electrochemomechanical strain of polypyrrole films under high tensile stresses, Jpn. J. Appl. Phys. (2009). https://doi.org/10.1143/JJAP.48.051506.

[30] T.N. Nguyen, K. Rohtlaid, C. Plesse, G.T.M. Nguyen, C. Soyer, S. Grondel, E. Cattan, J.D.W. Madden, F. Vidal, Ultrathin electrochemically driven conducting polymer actuators: fabrication and electrochemomechanical characterization, Electrochim. Acta. 265 (2018) 670–680. https://doi.org/10.1016/j.electacta.2018.02.003.

[31] K. Rohtlaid, G.T.M. Nguyen, C. Soyer, E. Cattan, F. Vidal, C. Plesse, Poly(3,4-ethylenedioxythiophene):Poly(styrene sulfonate)/Polyethylene Oxide Electrodes with Improved Electrical and Electrochemical Properties for Soft Microactuators and Microsensors, Adv. Electron. Mater. 5 (2019). https://doi.org/10.1002/aelm.201800948.

[32] L. Seurre, K. Rohtlaid, G.T.M. Nguyen, C. Soyer, S. Ghenna, S. Grondel, F. Vidal, B. Cagneau, C. Plesse, E. Cattan, Demonstrating Full Integration Process for Electroactive Polymer Microtransducers to Realize Soft Microchips, in: Proc. IEEE Int. Conf. Micro Electro Mech. Syst., 2020. https://doi.org/10.1109/MEMS46641.2020.9056371.

[33] T. Sugino, K. Kiyohara, I. Takeuchi, K. Mukai, K. Asaka, Actuator properties of the complexes composed by carbon nanotube and ionic liquid: The effects of additives, Sensors Actuators, B Chem. 141 (2009) 179–186. https://doi.org/10.1016/j.snb.2009.06.002.

[34] R.H. Baughman, Conducting polymer artificial muscles, Synth. Met. 78 (1996) 339–353. https://doi.org/10.1016/0379-6779(96)80158-5.

[35] Q. Pei, O. Inganäs, Electrochemical applications of the bending beam method. 2. Electroshrinking and slow relaxation in polypyrrole, J. Phys. Chem. 97 (1993) 6034–6041. https://doi.org/10.1021/j100124a041.

[36] F. Hu, Y. Xue, J. Xu, B. Lu, PEDOT-Based Conducting Polymer Actuators, Front. Robot. AI. 6 (2019) 1–17. https://doi.org/10.3389/frobt.2019.00114.

[37] F. Vidal, C. Plesse, D. Teyssié, C. Chevrot, Long-life air working conducting semi-IPN/ionic liquid based actuator, Synth. Met. 142 (2004) 287–291. https://doi.org/10.1016/j.synthmet.2003.10.005.

[38] N. Festin, C. Plesse, P. Pirim, C. Chevrot, F. Vidal, Electro-active Interpenetrating Polymer

Networks actuators and strain sensors: Fabrication, position control and sensing properties, Sensors Actuators, B Chem. 193 (2014) 82–88. https://doi.org/10.1016/j.snb.2013.11.050.

[39] P.S. Bass, L. Zhang, Z.Y. Cheng, Time-dependence of the electromechanical bending actuation observed in ionic-electroactive polymers, J. Adv. Dielectr. 7 (2017) 1–6. https://doi.org/10.1142/S2010135X17200028.

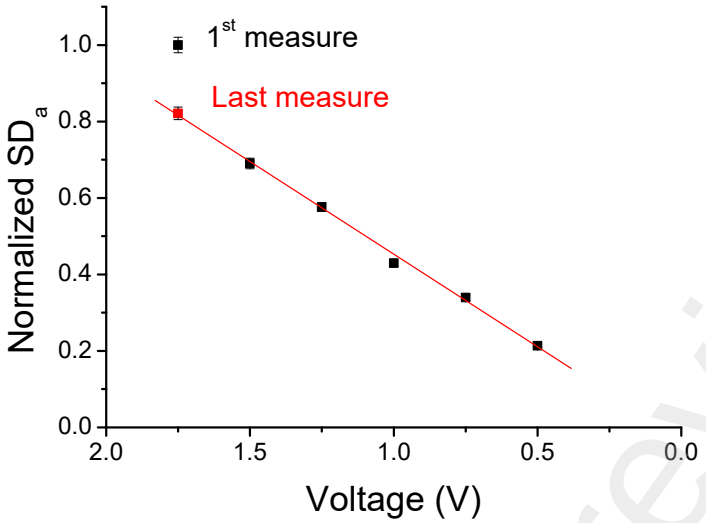

Figure S1: Normalized SD_a as a function of the voltage applied from 1.75 to 0.5 V, followed by a last measure at 1.75 V.

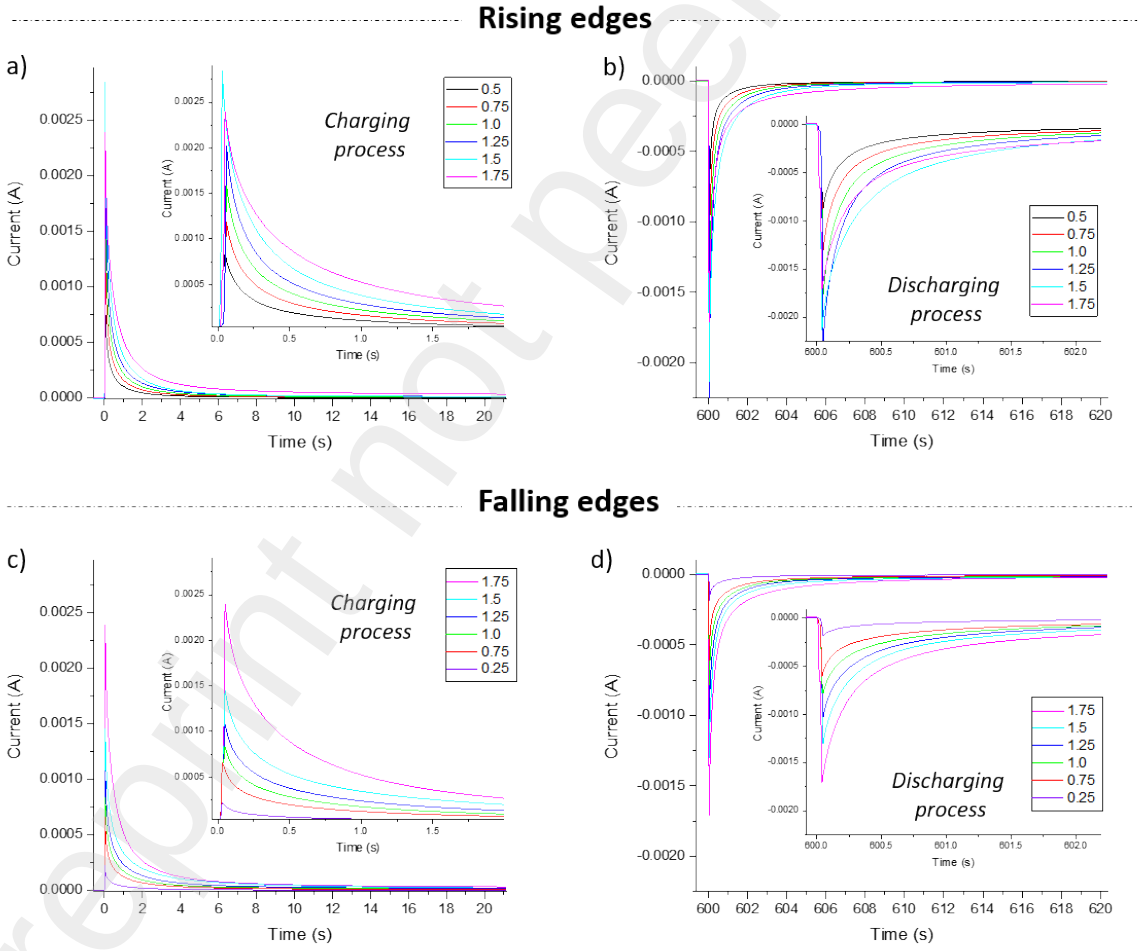

Figure S2: Current measurements as a function of time by increasing the voltage for a) charging and b) discharging processes, and by decreasing the voltage for c) charging and d) discharging processes.